

Article

Mesoscale Simulation of Year-to-Year Variation of Wind Power Potential over Southern China

Steve H.L. Yim ¹, Jimmy C.H. Fung ^{1,2} and Alexis K.H. Lau ^{1,3,*}

¹ Institute for the Environment, The Hong Kong University of Science and Technology, Hong Kong, China; E-Mails: steveyim@ust.hk; majfung@ust.hk

² Department of Mathematics, The Hong Kong University of Science and Technology, Hong Kong, China

³ Department of Civil and Environmental Engineering, The Hong Kong University of Science and Technology, Hong Kong, China

* Author to whom correspondence should be addressed; E-Mails: alau@ust.hk; Tel.: +852 - 2358 6944; Fax: +852 - 2358 1582

Received: 27 April 2009; in revised form: 27 May 2009 / Accepted: 1 June 2009 /

Published: 3 June 2009

Abstract: The objectives of this study are to combine historical observations and state-of-the-art numerical models (MM5/CALMET system) to map the spatial distribution of wind resources in high resolution, and to help foster a deeper understanding of the wind power potential over southern China (Guangdong). Hourly wind fields were simulated for three entire years (2004-2006). It found that almost 70% of the time, the wind speed along the coast of Guangdong is over 5 m/s, which is deemed a baseline magnitude for typical wind turbines. Spatial plots of the wind speed and power and their variations over Guangdong Province for the three years are also presented.

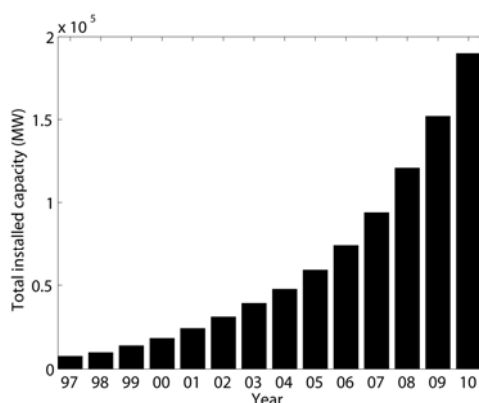
Keywords: wind power map; mesoscale modeling

1. Introduction

Wind energy is the fastest growing energy resource in the world and wind power is one of the most widely used alternative sources of energy today. Wind energy is clean, local, abundant, affordable,

inexhaustible and environmentally preferable. According to the World Wind Energy Association (WWEA), meeting the ever increasing global demand for electricity in the transition from the fossil fuels to renewable energy presents us with a daunting challenge. The significant body of evidence that supports global warming reveals that we are clearly living beyond environmental limits and consequently there have been calls by a number of leading authorities for considerable cuts in greenhouse gas emissions of up to 80% by 2050 [1]. In the same way as climate change is said to disregard national borders, strategies that seek to address this issue should also be international. Wind power has a significant role to play in reducing the global reliance on fossil fuels, helping to increase renewable energy's share in the global energy supply mix. Wind energy projects are, by their nature, environmental projects in that they are designed to develop clean and sustainable energy forms, energy that might otherwise come from fossil fuels associated with destructive impact on the environment and climate [1]. The global total installed capacity, as reported by the WWEA, is increasing, as it is shown in Figure 1. The total installed capacity in 1997 was 7,475 MW, in 2008 this rose to 121,188 MW and the prediction 2010 is up to 190,000 MW, which is an increase of more than 2,442% over the previous decade and a half [2].

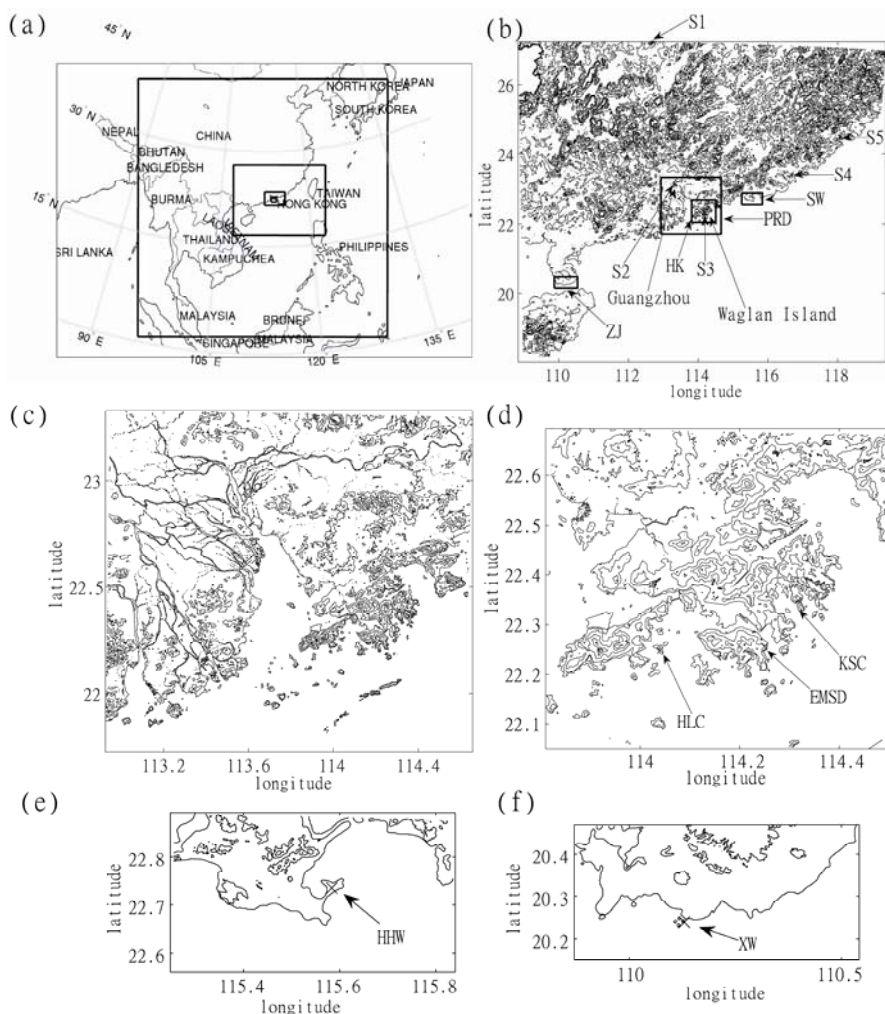
Figure 1. World wide total installed capacity (MW) and prediction from 1997 to 2010 reported by WWEA.



According to the Global Wind Energy Council (GWEC), 2008 was another year of breathtaking wind energy development in China, as the country's total installed capacity doubled for the fourth year in a row. New installed capacity totaled 6.3 GW in 2008, a 91% increase over the 2007 market. The country's cumulative wind power capacity in 2008 stands at 12.2 GW while 1.26 GW in 2005, making China the fourth largest wind market in the world. The prospects for future growth in the Chinese market are very good. In response to the financial crisis, the Chinese government has identified the development of wind energy as one of the key economic growth areas, and in 2009, new installed capacity is expected to nearly double again. At this rate, China is on its way to overtake Germany and Spain to reach second place in terms of total wind power capacity in 2010. This means that China would have met its 2020 target of 30 GW ten years ahead of time [3]. Therefore, wind energy will play an important role in the global, and in particularly, China's, move towards a sustainable future and work to identify favorable locations needs to be undertaken in the near future to support this key source of renewable energy. However, studies of wind power potentials over Guangdong are very limited.

The best estimate of wind power potential is the long-term wind record at the site where the turbines are to be installed, but this information is rarely available. Traditionally, the conventional method of estimating wind potential is to interpolate data from wind measurements taken at nearby monitoring sites. However, unless the terrain is flat and the land-surface characteristics are uniform, the distance over which existing wind information is useful is quite limited. Fung *et al.* [4] and Li *et al.* [5] investigated the wind power over HK by using 1-year measured data on from Lantau Island and Waglan Island respectively. Lu *et al.* [6] studied the potential and feasibility of large-scale offshore wind power for the HK region by analysing 1-year of wind data measurements on Waglan Island. Zhou *et al.* [7] investigated the wind power potential in the PRD by analysing wind data measurements at four islands along the PRD coastal line. However, these authors only utilised measurement data at few points to investigate the wind power potential in a region with highly complex terrain. This heterogeneous complicated terrain means that it is unlikely that these studies are representative of the wind power across the entire region.

Figure 2. (a) Four nested domains used in MM5 (solid lines); resolutions from outer-most to innermost domains are 40.5, 13.5, 4.5 and 1.5 km. (b) Computational domain of GD in CALMET and shaded contours representing complex topography. Black boxes in (b) shows computational domains of (c) PRD, (d) HK, (e) Zhan Jiang (ZJ) and (f) Shan Wei (SW). The contour lines levels (in metres) are 0, 100, 300, 500, 700 and 900.



Therefore, numerical methods with high resolution grids are needed. Model simulations can produce 3D descriptions of wind field characteristics that cannot be obtained from extensive field measurements. They can describe the changes induced on the wind field from the topography and land cover variations. In this study, the PSU/NCAR mesoscale model (known as MM5) is coupled with the diagnostic model CALMET (MM5/CALMET system) to estimate the detailed wind resources in Guangdong Province (GD), Pearl River Delta (PRD) and Hong Kong (HK) (see also Figure 2).

This system was run on an hour-to-hour basis, first by using MM5 to generate a large-scale wind field as a first guess field, and then utilizing the CALMET model to adjust the meteorological fields to reflect the high-resolution terrain and land use data to produce wind fields at a resolution of 3 km for GD, 250 m for PRD and 100 m for HK. Three years of data (2004, 2005 and 2006) were simulated in this study. The main advantage of this approach is that it provides detailed temporal as well as spatial variations in the wind field for the study areas, which is not possible when the data are forced with only mean conditions. This is particularly important for southern China where the wind variability is considerable.

In Section 2, we describe how the model was set up and shows the comparison of model and observational results. In Section 3, results on wind availability over the study area and the Weibull density function and the wind power map are discussed. Conclusions will be drawn in Section 4.

2. Methodology

2.1. The Prognostic Mesoscale Model, MM5

The meteorological model used in this study is the Pennsylvania State University (PSU) - National Center for Atmospheric Research (NCAR) Fifth-Generation Mesoscale Model (MM5) version 3.6.3. MM5 is a prognostic model in which primitive equations that govern the state of the atmosphere are solved. It is a limited-area, non-hydrostatic model with terrain-following sigma-coordinates [8,9].

In this study, MM5 was configured with four two-way interactive nested grids (Figure 2a). The outermost domain (D1) extends from central China (north) to the Philippines (south) and covers most of southeastern China and the South China Sea to provide the boundary conditions for the intermediate domains, D2 and D3, both of which have important influences on the weather of Hong Kong and its vicinity. The D1 domain had 115 x 119 grid points with a horizontal resolution of 40.5 km. The intermediate domains, D2 and D3, contain 127 x 97 grid points with a horizontal resolution of 13.5 km and 85 x 55 grid points with a horizontal resolution of 4.5 km, respectively. The innermost domain, D4, encompasses the whole territory of Hong Kong and has 67 x 58 grid points with a horizontal resolution of 1.5 km. MM5 is written with a terrain-following (or sigma) coordinates and each σ level is defined by $\sigma = (P - P_{top}) / (P_{sur} - P_{top})$, where P_{sur} is the surface pressure, with the pressure at the model top, $P_{top} = 100$ hPa. According to the literature, the model top is usually defined as 100 hPa, see [10-15]. It should be high enough to capture all the weather-related process for this study concerns, thus this value is chosen as our model top. In the vertical direction, 34 sigma levels were defined unequally from the ground to the model top, with the first 10 layers (which corresponding to the physical heights of 8.5 m, 27 m, 53 m, 88.5 m, 131.5 m, 182 m, 256 m, 352 m, 531 m and 933 m)

being concentrated in the atmospheric boundary layer (about 1.0 km above the ground level) to resolve the detailed structure of the planetary boundary layer.

In the literature, different parameterization schemes were applied to the study over southern China. Wang *et al.* [10] applied MRF PBL scheme [16], Kain-Fritsch cumulus parameterization scheme and Reinsier2 Radiation in their study. The high-resolution Blackdar Scheme, Kain-Fritsch 2 cumulus parameterization scheme and RRTM longwave scheme were applied by Ding *et al.* [17]. In our current MM5 simulations, the medium-range forecast (MRF) planetary boundary layer scheme [16] and RRTM longwave scheme are applied to all four domains, while the Grell cumulus parameterization scheme is used in D1 and D2 but not in the rest domains as recommended by [9].

Four-dimensional data assimilation (FDDA) was employed to improve the accuracy of the meteorological simulation [18]. Four-dimensional data assimilation (FDDA) is to combine the current and past data in the model's prognostic equations to provide time continuity and dynamic coupling among the various fields. In FDDA procedure, the method of Newtonian relaxation or nudging relaxes the model state toward the observed state by adding, to one or more of the prognostic equations, artificial tendency terms based on the difference between the two states. The model solution can be nudged toward either gridded analyses or individual observations during a period of time surrounding the observations. The detailed description is shown in [18].

In the present study, multiple MM5 simulations are performed with the length of each simulation not extending beyond a four-day period for each of the four nested domains with two-way nesting boundary conditions. The first 24 hours of each run was discarded as a spin-up run, i.e., each simulation overlaps the previous simulation to account for model spin-up time. Up to 121 separate MM5 simulations are required to build a one-year data set of the meteorological fields. Initial conditions and boundary conditions were provided by the 1.0 degree National Centers for Environmental Prediction (NCEP) Final Analyses (FNL) at six-hour intervals.

The ability of the current MM5 setup to simulate the surface winds (both speed and direction) was evaluated using a statistical method and wind observations from the Hong Kong Observatory. The statistical parameters examined include observed and predicted means, standard deviations, root-mean-square difference for wind speed, and indices of agreement for wind speed and wind direction. The mean value of RMSE is 0.93 while the mean Index of Agreement is 0.78. These results indicated that the MM5 agrees well with the observed values. Details of the evaluation are presented in [14,15,19].

2.2. The CALMET Diagnostic Meteorological Model

In this study, the PSU/NCAR mesoscale model (known as MM5) is coupled with the diagnostic model CALMET (MM5/CALMET system) to estimate the detailed wind resources in Guangdong Province (GD), Pearl River Delta (PRD) and Hong Kong (HK).

CALMET is a diagnostic meteorological model that develops hourly wind fields on a three-dimensional gridded modeling domain. The diagnostic wind field module uses a two-step approach in the computation of wind fields [20]. In the first step, the wind field outputs from the MM5 model are ingested by the CALMET model as an initial-guess wind field, i.e., the prognostic winds are interpolated in the fine-scale CALMET grid. In second step, the normal diagnostic adjustments for the fine-scale kinematic effects of terrain, slope flows and terrain blocking effects are made to produce a

Step-1 wind field. The kinematic effects of the terrain on the horizontal wind components are evaluated by applying a divergence-minimization procedure to the initial guess of the wind field. Finally, an objective analysis procedure is employed using all available surface and upper-level observational data.

In this study, CALMET was configured with five domains (Figures 2b-f) with 10 layers which corresponding to the physical heights of 10 m, 30 m, 60 m, 120 m, 230 m, 450 m, 800 m, 1250 m, 1850 m and 2600 m. The outermost domain (D1) covers whole GD. Domain 2 (D2) covers whole Pearl River Delta and Domain 3 (D3) covers whole Hong Kong. Domain 4 (D4) and Domain 5 (D5) are set to do the validations of the model and cover the locations of field measurements which are located in Hung Hai Wan (HHW) and Xu Wen (XW). These regions have complex small-scale terrain features (see Figure 2) as well as sharp gradients in land surface characteristics that are smaller than the typical resolutions used in MM5 simulations (around 1-4 km [21-24]). The result of this is that the effects of the terrain and land surface characteristics on the meteorological fields are not always captured in the MM5 simulations. It also found that the coupling of MM5 with CALMET can resolve more realistic wind field [21,25]. Truhetz *et al.* [26] investigated the influence of MM5's horizontal grid spacing on the resultant wind fields and found that the quality of the initial wind fields of the diagnostic model is of vital importance for the resultant wind field. Since very high vertical wind components during model testing accompanied by unrealistic horizontal components. Thus, in order to improve this insufficiency, MM5/CALMET system with fine resolutions (3 km for GD, 250 m for PRD and 100 m for HK) was utilized in this study.

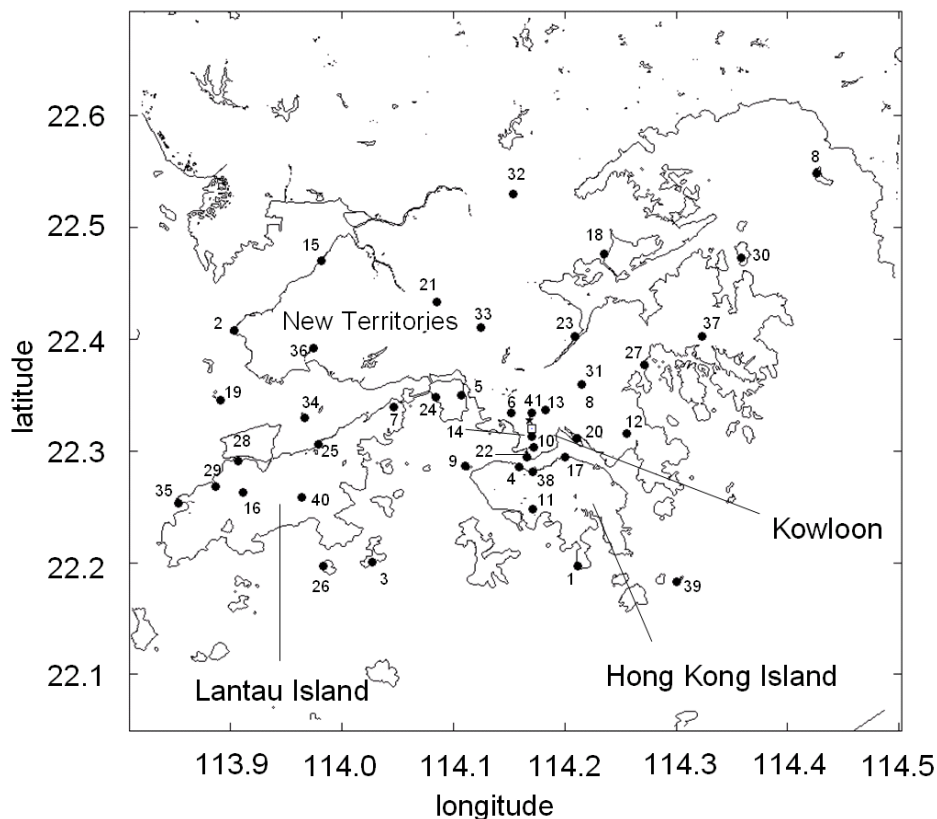
CALMET reads hourly surface observations of wind speed, temperature, cloud cover, ceiling height, surface pressure, relative humidity, and precipitation. The upper air observations required by CALMET include vertical profiles of wind speed, wind direction, temperature, pressure, and elevation. In order to improve the initialization of the diagnostic model, hour-by-hour wind field in MM5 prognostic model with 1.5 km resolution are ingested by CALMET as the initial-guess wind field. This step is expected to improve the model's performance by providing equally spaced data points both at the surface and upper levels within the modeling domain where observational data are not available [21].

2.3. Model validation

2.3.1. Comparison of Surface Stations and Upper Sounding Data

A set of common statistical parameters [27,28] were employed to evaluate the performance of the model simulation and compare the differences between the model results and observations at the surface stations. The locations of the surface stations are shown in Figure 3.

Figure 3. Forty-one meteorological stations operated by the Hong Kong Observatory as indicated by •. The digits represent different stations and their corresponding names of the stations are given in Table 1. The small square (station 14) is the King’s Park upper air sounding station and the small star is the Sham Shui Po wind profiler station.



Statistical parameters used to evaluate the model performance include the observed and predicted means, the standard deviation (*SD*), the root mean square error (*RMSE*) and the index of agreement (*I*) for wind speed at 10 m above the ground. The root mean square error is defined as:

$$RMSE = \left[\frac{1}{N} \sum_{i=1}^N (p_i - o_i)^2 \right]^{1/2} \tag{1}$$

where p_i and o_i are the simulated and observed values, respectively, for measurement i . N represents the total number of measurements. The index of agreement is defined as:

$$I = 1 - \frac{\sum_{i=1}^N (p_i - o_i)^2}{\sum_{i=1}^N (|p_i - \bar{o}| + |o_i - \bar{o}|)^2} \tag{2}$$

where \bar{o} denotes the average observed wind. A model index value of 1 indicates perfect agreement between the model and observations while an index of 0 indicates no agreement. Table 1 shows the performance statistics results for the assimilated stations (20040101-20041231). The index of agreement shows that the model results matched the observational data quite well.

Table 1. The statistical results of 41 included meteorological surface stations.

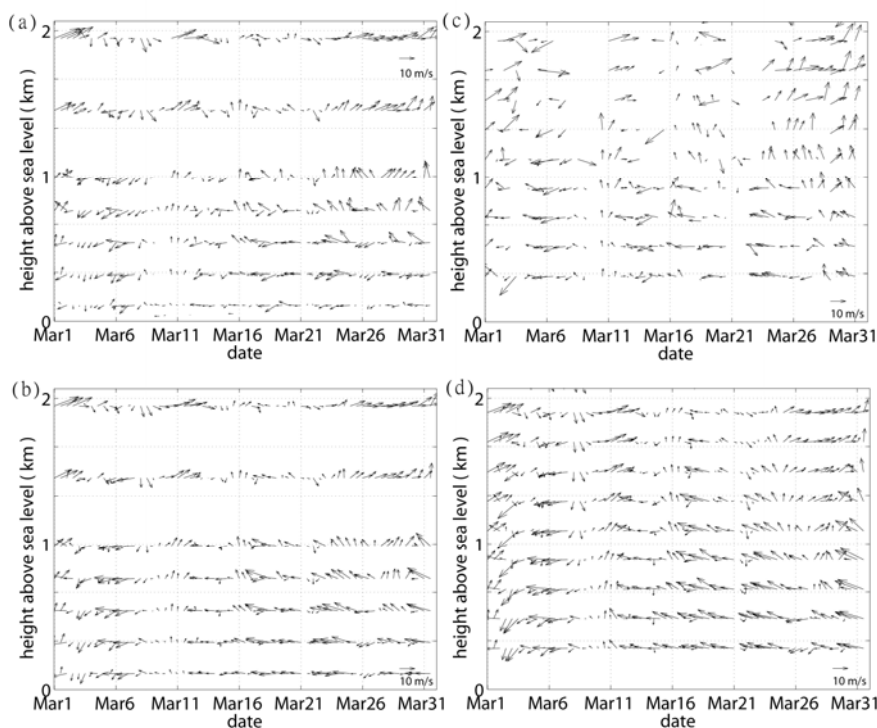
Station name	Observed Mean Speed (m/s)	Model Mean Speed (m/s)	Observed SD	Model Result SD	RMSE	I	% of valid data
1 Bluff Head (BHD)	3.67	3.53	1.98	1.72	0.41	0.9	95.3
2 Black Point (BPT)	3.06	2.92	2.42	2.04	0.52	0.9	93.6
3 Cheung Chau (CCH)	5.00	4.79	2.51	2.53	0.27	0.9	90.8
4 Central: Star Ferry Pier (CEN)	2.97	3.03	1.74	1.72	0.35	0.9	99.6
5 Ching Pak House, Tsing Yi (CPH)	3.76	3.26	1.60	1.47	0.39	0.9	99.5
6 Cheung Sha Wan (CSW)	2.49	2.63	1.15	1.21	0.45	0.9	99.6
7 East Lantau (ELN)	3.93	3.81	2.21	2.12	0.18	0.9	99.2
8 Ping Chau (EPC)	1.44	2.77	0.84	1.98	0.18	0.9	88.9
9 Green Island (GI)	6.15	5.83	3.35	3.23	0.18	0.9	96.5
10 Hong Kong Observatory (HKO)	2.93	3.35	1.69	1.91	0.77	0.9	99.0
11 Wong Chuk Hang (HKS)	2.85	2.67	1.55	1.44	0.18	0.9	99.6
12 Tseung Kwan O (JKB)	1.85	1.93	0.98	1.19	0.22	0.9	99.7
13 Kowloon Tsai (KLT)	2.46	2.56	1.13	1.45	0.86	0.8	99.1
14 King's Park (KP)	3.09	3.73	1.32	2.21	1.76	0.7	79.2
15 Lau Fau Shan (LFS)	3.21	3.21	1.58	1.59	0.09	0.9	99.8
16 Nei Lak Shan (NLS)	7.14	6.93	4.03	3.64	0.79	0.9	97.7
17 North Point (NP)	4.09	3.40	1.80	1.53	0.76	0.9	99.9
18 Tai Mei Tuk (PLC)	4.05	3.98	2.07	2.11	0.21	0.9	97.6
19 Sha Chau (SC)	5.62	5.45	2.67	2.74	0.10	0.9	98.4
20 Kai Tak (SE)	3.65	3.01	1.50	1.33	0.68	0.9	94.0
21 Shek Kong (SEK)	3.19	2.73	1.64	1.40	0.38	0.9	98.9
22 Star Ferry: Tsim Sha Tsui (SF)	3.55	3.74	2.06	2.25	0.50	0.9	99.6
23 Sha Tin (SHA)	2.53	2.34	1.07	1.07	0.45	0.9	99.5
24 Shell Tsing Yi Installation (SHL)	2.52	2.44	1.59	1.50	0.16	0.9	99.3
25 Siu Ho Wan (SHW)	3.82	3.62	2.15	1.87	0.80	0.9	80.3
26 Shek Kwu Chau (SKC)	5.37	4.61	2.81	2.26	0.98	0.9	69.8
27 Sai Kung (SKG)	2.97	2.70	1.93	1.66	0.46	0.9	99.8
28 Sha Lo Wan (SLW)	3.61	3.57	2.32	2.28	0.23	0.9	98.6
29 Sham Wat (SW)	2.55	2.79	1.36	1.68	0.24	0.9	98.9
30 Tap Mun (TAP)	3.20	3.18	1.74	1.79	0.15	0.9	99.7
31 Tate's Cairn (TC)	6.57	4.97	3.21	2.19	1.93	0.8	98.0
32 Ta Kwu Ling (TKL)	2.59	2.49	1.38	1.38	0.07	0.9	99.8
33 Tai Mo Shan (TMS)	5.80	5.99	3.10	3.05	0.62	0.9	99.6
34 Tai Mo To (TMT)	4.80	4.66	2.31	2.25	0.17	0.9	97.6
35 Tai O (TO)	4.46	4.00	3.54	3.16	0.23	0.9	97.4
36 Tuen Mun (TUN)	2.60	2.51	1.38	1.20	0.28	0.9	89.0
37 Tsak Yue Wu (TYW)	1.78	1.89	1.66	1.56	0.14	0.9	98.7
38 Wan Chai (WCN)	4.65	4.55	2.36	2.49	0.29	0.9	99.7
39 Waglan Island (WGL)	6.82	6.17	3.12	3.25	0.08	0.9	97.3
40 Yi Tung Shan (YTS)	7.16	6.96	3.63	3.45	0.68	0.9	98.4
41 Yau Yat Chuen (YYC)	2.81	3.08	1.90	1.93	0.85	0.9	98.7

Data from three surface stations and one upper-level sounding station were not ingested into the CALMET model and the data were then compared with that of the model simulation values. The comparisons for the surface station data (20040101-20041231) are shown in Table 2. The statistics information reveals the satisfactory ability of the models to reproduce the wind field. The results of upper sounding (please refer to Figure 3 for the location) comparison (20040301-20040330) are also shown in Figure 4 and the results are also favorable, for details please refer to [25].

Table 2 The statistical results of three meteorological surface stations not ingested in CALMET.

Station name	Observed Mean Speed (m/s)	Model Mean Speed (m/s)	Observed SD	Model Result SD	RMSE	I	% of valid data
1 Tuen Mun (TUN)	2.60	2.86	1.38	1.53	1.15	0.84	89.0
2 Cheung Sha Wan (CSW)	2.41	3.06	1.17	1.77	1.38	0.77	99.6
3 Cheung Chau (CCH)	5.02	4.32	2.51	2.47	1.30	0.93	90.8

Figure 4. Comparisons of vertical wind fields. (a) King’s Park upper air sounding data (data available at every 12 hours UTC00 and UTC12) and (b) corresponding time CALMET model results at King’s Park; (c) Sham Shui Po wind profiler data (data available at every 12 hours UTC00 and UTC12) and (d) corresponding time CALMET model results at Sham Shui Po.



2.3.2. Comparison of Field Data

Three other locations in Hong Kong and two other locations in Mainland China with upper level wind data were used to do further model verifications with the upper level winds. These stations are:

- (1) One station from the Electrical and Mechanical Services Department (EMSD) in HK
- (2) Two stations from China Light Power (CLP) in HK
- (3) One station in Hung Hai Wan (HHW) in Shan Wei(SW) (China)
- (4) One station in Xu Wen (XW) in Zhan Jiang(ZJ) (China)

A temporary wind monitoring station in Pottinger Peak was located in eastern coastal region of Hong Kong Island and was maintained by Electrical and Mechanical Services Department for one year (20041001-20050930) as shown in Figure 2d. The monitoring structures, measuring 50 m in height, were equipped with anemometers at different elevations to gather data for assessment. A 12-month wind monitoring cycle is considered appropriate to determine the diurnal and seasonal variability of the wind regime at the studied locations. Additionally, Figure 2d also shows the locations of the two CLP monitoring stations with measuring height at 30 m and 50 m respectively, Kau Sai Chau (KSC) (20060428-20060724) and Hei Ling Chau (HLC) (20051110-20060731) in Hong Kong, Figure 2e shows the location of Hung Hai Wan (HHW) (60 m above ground and 20060501-20061231) along the western coast of Guangdong Province and Figure 2f shows the location of Xu Wen (XW) (60 m above ground and 20060501-20061231) along the eastern coast of Guangdong Province. The comparison between the observational data and the model simulation is quite good. The simulation is able to capture the large fluctuations of the wind speed as shown in Figure 5. The statistical parameters are also measured and shown in Table 3.

Figure 5. Comparison of hourly model results (red) and observational data (blue) at (a) Pottinger station maintained by EMSD, (b) HLC station maintained by CLP, (c) KSC station maintained by CLP, (d) Hung Hai Wan (HHW) and (e) Xu Wen (XW).

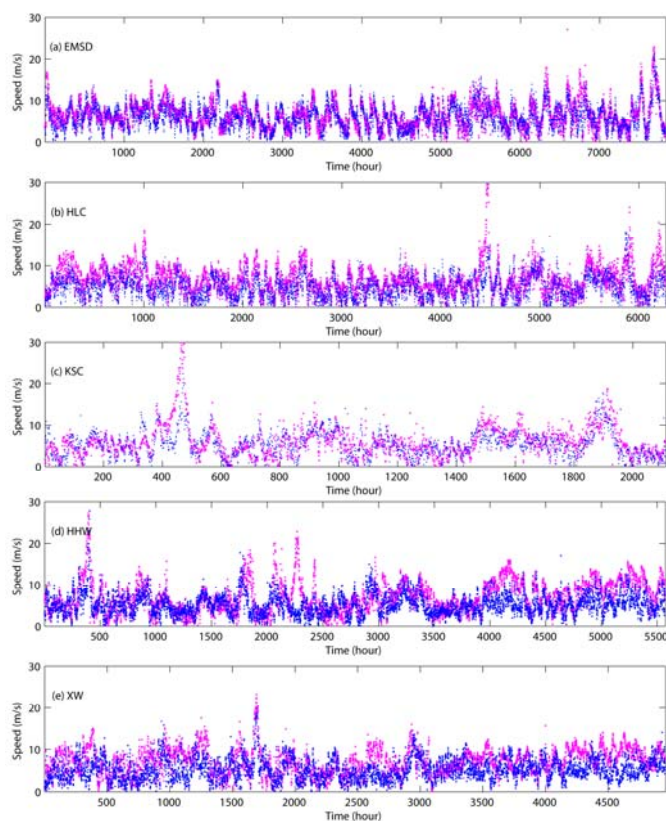


Table 3. The statistical results of five field data stations.

Station name	Observed Mean Speed (m/s)	Model Mean Speed (m/s)	Observed SD	Model Result SD	RMSE	I	% of valid data
1 EMSD	5.95	6.53	2.91	3.02	1.32	0.75	88.2
2 Hei Ling Chau (HLC)	4.80	5.46	2.71	2.41	1.36	0.70	97.0
3 Kau Sai Chau (KSC)	5.40	5.90	3.08	3.78	1.12	0.75	96.8
4 Hung Hai Wan (HHW)	5.25	6.10	2.57	3.75	1.47	0.60	95.5
5 Xu Wen (XW)	5.28	6.00	2.54	3.02	1.54	0.63	86.9

The model-error may be due to the limitation of CALMET model that its performance depends upon the density, frequency, and accuracy of the observations used as input for computing wind fields [29]. But, on average, these results show that CALMET with a high-resolution grid, coupled with MM5 input is able to reproduce the general features of the spatial and the vertical structure of the wind over Guangdong Province.

3. Results and Discussions

3.1 Wind Availability over Study Area

Comprehensive understanding of wind conditions over the assessment area for wind power generation is essential, especially for regions where the topography is complex. As shown in Figure 2b, the topography of Guangdong Province is particularly complicated, thus, it is important to grasp the intricacies of the detailed wind pattern.

In this study, three years (2004-2006) worth of wind field simulations were studied. In order to exam how representative the three studied years of data is on a longer temporal scale, longer period data from five Global Telecommunication System (GTS) stations and one automatic Hong Kong Observatory weather station - Waglan Island (WGL) located in Guangdong (see Figure 2b) is plotted. The wind data of stations (S2,S3,S4,S5,WGL) can be regarded as the background prevailing wind condition for the South China Sea since these stations are sited along the coast facing the South China Sea without any obstruction while S1 represents the inland region.

Figure 6 shows that the weather data used in this study is typical of the longer trend. The prevailing wind conditions from South China Sea are relatively steady with the maximum variation of annual mean, less than 10% from 2004 to 2006. From this figure, it shows that values for 2005 and 2006 are around the mean and 2004 is slightly below the mean.

Figure 7 shows the annual mean wind speed over Guangdong Province in 2004, 2005 and 2006. It is obvious that the high wind velocities – between 5 and 6 m/s are normally located on hilltops or in coastal areas. Although the wind speed on hilltops can be up to 8 m/s at 60 m above ground, hilltops are not always suitable for wind power generation. Construction of wind turbines on hilltops is a difficult task and many problems have to be solved, for example the cable connections to the main grid. In contrast, wind resources in coastal areas are extremely valuable. In general, 5 m/s is regarded as the baseline wind necessary because the average cut-in wind speed of many typical commercial

wind turbines is around 4-5 m/s. Furthermore, it shows that the wind speed along the coastal areas is often over 5 m/s which is deemed a good enough wind resource to generate an acceptable supply of wind power. Figure 8 shows the frequency of wind speed ≥ 5 m/s over Guangdong Province. Almost 70% of the time in a year, the wind speed along coastal line is over the typical cut-in speed of the wind turbines.

Figure 6. Annual mean wind speed of 5 GTS stations and HKO station (Waglan Island) from 1993 to 2008, see Figure 2 for exact locations.

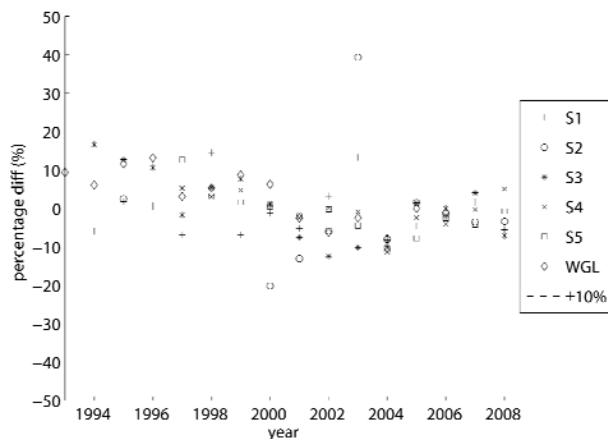


Figure 7. Annual mean wind speed at 60 m above ground over GD in (a) 2004, (b) 2005 and (c) 2006.

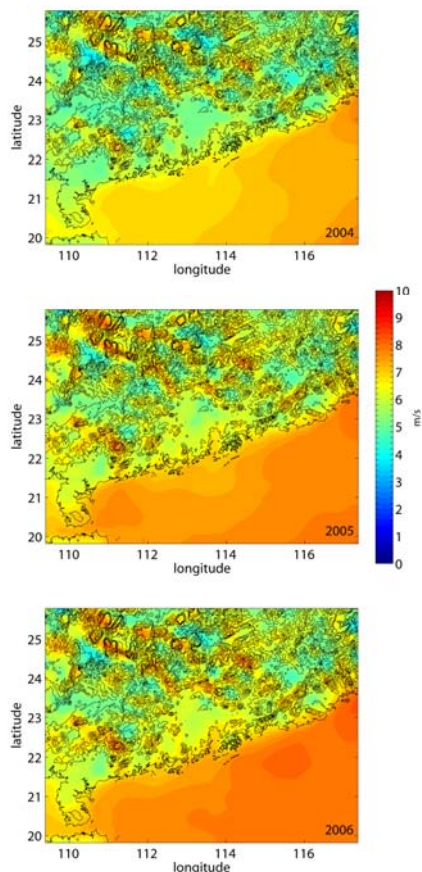
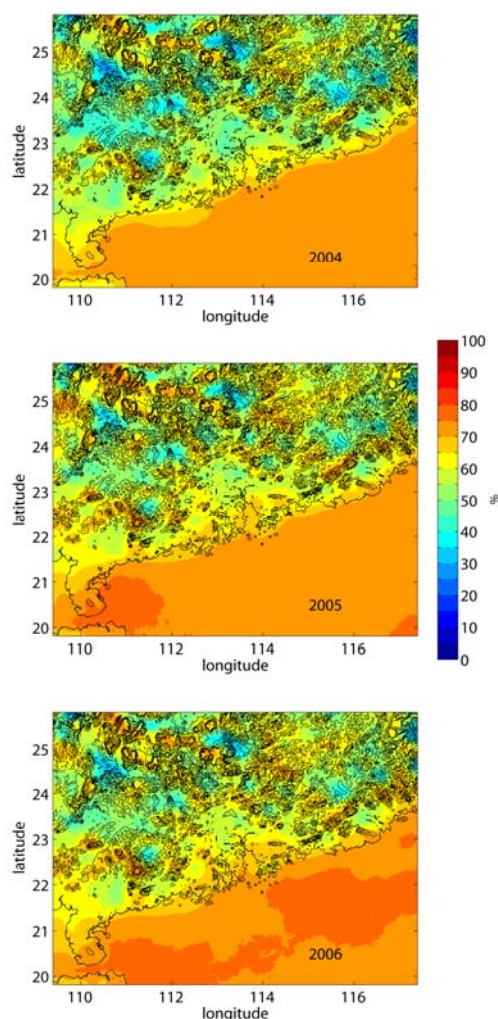


Figure 8. Frequency of wind speed ≥ 5 m/s over GD in (a) 2004, (b) 2005 and (c) 2006.



The variation of wind speed over longer, annual time scales is also an important parameter for wind power generation. Figure 7 helps us to understand the variation of the wind speed from 2004 to 2006. Clearly, the availability of wind speed inland is less than in coastal areas.

By examining the percentage difference for Guangdong coastal areas (not plotted here), the difference from 2004 to 2006 in wind speed is approximately 20%. Wind availability along coastal area also increases which is beneficial for wind power.

Wind power assessment should not only consider the mean wind speed, but also the wind characteristics and wind speed spectrum [25] and this is discussed in the following section.

3.2. Weibull Function, Wind Map and Wind Power

A thorough understanding of the characteristics of the wind regime in which a wind turbine is expected to work is a pre-requisite for the successful planning and implementation of any wind power project. Knowledge of wind velocity distribution at different time scales and the quantity of power associated with these wind spectra are essential for the proper sizing and siting of a wind project. It is established [7] that the Weibull distribution can be used to characterize wind regimes in terms of the wind's probability density and cumulative distribution functions. If wind speeds were measured

throughout a year, it would find that in most areas strong gale force winds are rare, while moderate winds are quite common. The variations in wind speed are best described by the Weibull probability distribution function with two parameters – shape (k) and scale (c) parameters. The probability of the wind speed being v during any time interval is:

$$f(v) = \frac{k}{c} \left(\frac{v}{c}\right)^{k-1} \exp\left(-\left(\frac{v}{c}\right)^k\right) \quad (k > 0, v > 0, c > 1) \quad (3)$$

where c is the scale parameter, in the units of the speed and k is the shape parameter. Once the mean and variance of the wind speed are known, the following approximation can be used to calculate the Weibull parameters, c and k :

$$k = \left(\frac{\sigma}{\bar{v}}\right)^{-1.086} \quad (1 \leq k \leq 10) \quad (4)$$

$$c = \frac{\bar{v}}{\Gamma(1 + 1/k)}, \quad (5)$$

where:

$$\bar{v} = \frac{1}{n} \sum_{i=1}^n v_i \quad \text{and} \quad \sigma^2 = \frac{1}{n-1} \sum_{i=1}^n (v_i - \bar{v})^2 \quad (6)$$

Here, Γ is the gamma function. The shape (k) and scale (c) parameters can be calculated according to equations 4 and 5 respectively. In addition, for the analysis of the wind power potential, the corresponding percentage difference can be as large as 50% between considering the mean wind speed only and considering the wind speed spectrum [25]. This is because the power density is determined not only by the mean speed but also by the distribution of the wind speed. In general, the mean wind speed should not be used to calculate the wind power density because the error can be quite large. This result also indicates the importance of incorporating the variation into the wind power potential during diurnal cycles [30].

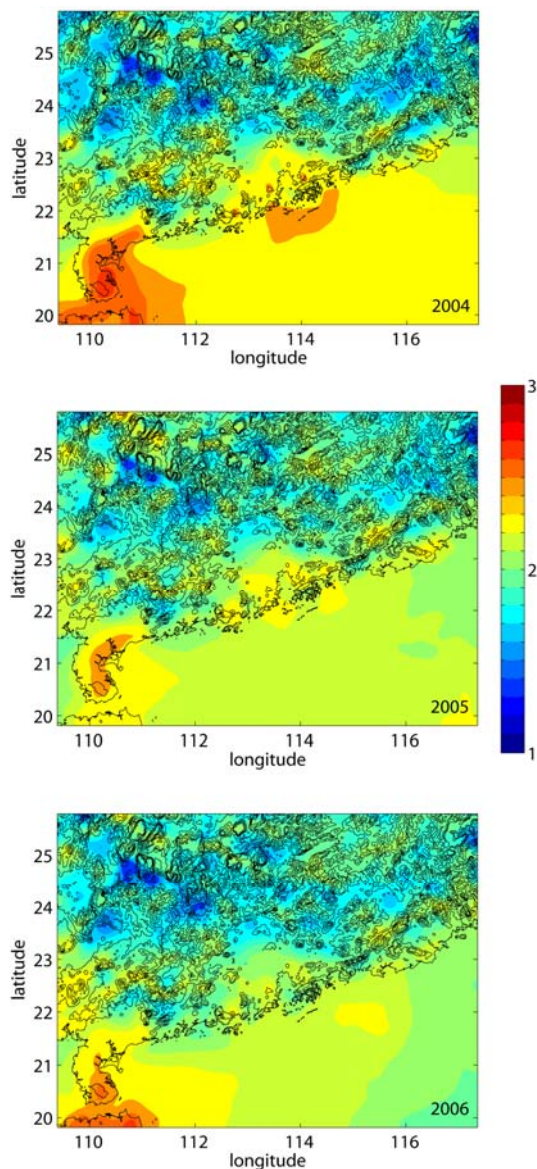
In general, at least one year of measurement data from an observation station or simulation data are required in order to determine the wind power potential. Of course, it is preferable to have wind speed data at least five to ten years, if the data are available. However, for this study, our main purpose was to demonstrate that the CALMET system coupled with MM5 can be used to estimate the detailed wind resources in Guangdong Province. Therefore, the simulation was conducted for three years due to limited computational resources.

3.2.1. The Weibull Density Function in Guangdong Province

Figures 9a-c show the shape parameter k in Guangdong Province in 2004, 2005 and 2006, respectively. Along the coastal region, most of the values of the shape parameter k are around 2.4 rather than 2. In terms of wind, the higher values of the shape parameter represent a situation in which a majority of the data is concentrated around the mean with fewer extreme values. For low wind speed situations, it is not worthwhile, nor efficient, to engage the turbine if the wind speed is below the cut-in speed. For high wind speed situations beyond a certain wind speed (cut-out speed), such as may occur during gusts, the rotor is shut off to protect the blades, electrical generator, and other components of the system [31]. When the shape parameter is higher than 3, the wind distribution approaches the

normal distribution, often called the *Gaussian* distribution. Under this situation, the relatively stable wind speeds provide ideal conditions for wind turbine operation.

Figure 9. Shape parameter k at 60 m above ground over GD in (a) 2004, (b) 2005 and (c) 2006.



The shape parameters around Guangdong Province typically vary between 1.5 and 2.5. For a typical commercial wind turbine (for example, the Vestas V66 2000KW manufactured by Vestas) the two extreme values of the shape parameter k (1.5 and 2.5) can have a 14% difference in wind power. Therefore, the influence of the shape parameter k cannot be ignored when evaluating wind power potential.

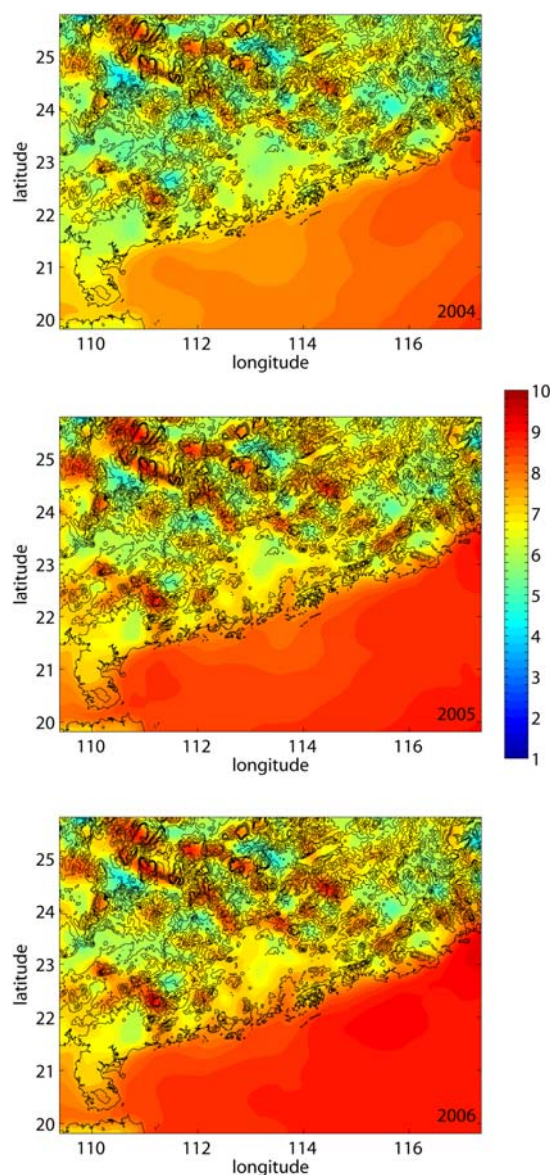
As expected, the value of the k is less than 2 (blue colour) in most inland parts of Guangdong Province (except at the top of the mountains). These values represent weaker wind situations. In some areas, the values are lower than 1.5, i.e. these areas are not suitable for wind power. However, around the coastal region of Guangdong Province and the Pearl River Delta region, the values of k are above

2, representing that the wind speed spectrum shifts to mean wind speed values that provide stable wind supply for wind turbines.

Besides the shape parameter k , the influence of the scale parameter c should also be taken into account. The scale parameter c is directly proportional to the mean wind speed for a given value of the shape parameter k ($1 < k < 3$). Therefore the scale parameter c can be interpreted as the velocity parameter providing $1 < k < 3$.

Figures 10a-c show the scale parameter c in Guangdong Province in 2004, 2005 and 2006 respectively. This parameter indicates the annual variation in wind speed. It found that the variation of the scale parameter c over inland regions is quite small. It changes around 0.5 from 2004 to 2006. In contrast, the scale parameter c varies significantly in coastal areas and the variation was up to 1 from 2004 to 2006. Based on these results, it can conclude that the coastal areas have good wind power potential but variation can be as large as 40–50%.

Figure 10. Scale parameter c (m/s) at 60 m above ground over GD in (a) 2004, (b) 2005 and (c) 2006.



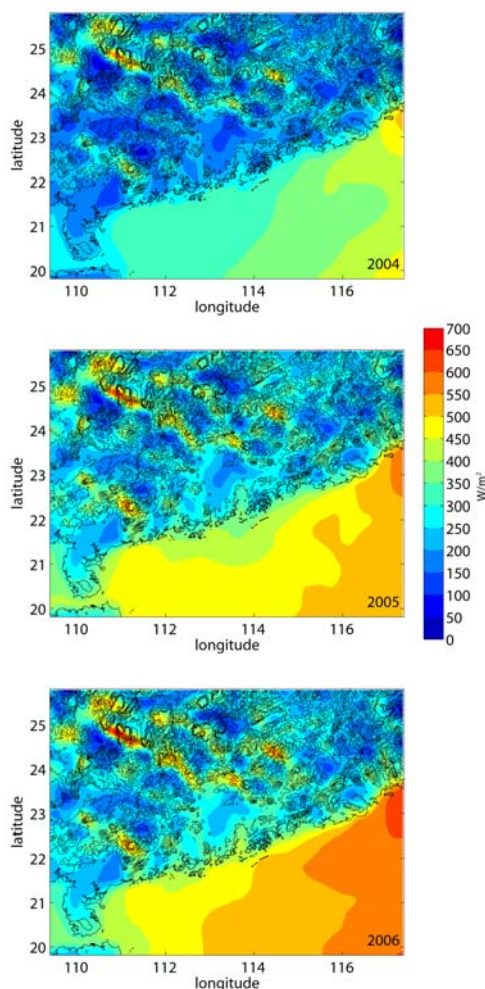
3.2.2. Annual Average Wind Power

Once the shape (k) and scale (c) parameters are found, the annual wind power can be calculated according to Equation (7). If $f(v)$ is the Weibull probability distribution of v , the average power of the wind, \bar{P}_d , can be expressed by:

$$\bar{P}_d = \frac{1}{2} \rho(z) A \int_0^{\infty} v^3 f(v) dv = \frac{\rho(z) A \bar{v}^3 \Gamma(1 + 3/k)}{2[\Gamma(1 + 1/k)]^3}. \quad (7)$$

where \bar{v} is the average wind speed, $\rho(z) = \rho_0 e^{-z/H}$ is the density of air at different heights, H is the scale height, ρ_0 is air density at sea level, and the wind swept area is defined by A in m^2 . The wind power is commonly calculated in watts per square meter, W/m^2 .

Figure 11. Wind power per unit area in (a) 2004, (b) 2005 and (c) 2006 at 60 m above ground over GD.



Figures 11a-c show the wind power per unit area in 2004, 2005 and 2006 at 60 m above ground over Guangdong Province. Besides the hilltops, the wind resources are generally concentrated along coastal areas. It can be seen that within these three years, the variation of wind power is not consistent across the study area. By examining the percentage difference in wind power within the study area (not plotted here), it found that the difference in wind power between the three years, 2004, 2005 and 2006,

decreases when moving from the coastal areas to inland areas. For the coastal areas, the wind power in 2004 is obviously lower when compared with 2005 and 2006 and this is especially true in Guangzhou. The difference is up to 40-50% between 2004 and 2006, whereas the wind power in 2005 and 2006 is more similar (within 20%). In these figures, they also show the wind power potential with the highest values (500-600 W/m²) along the coast of Guangdong Province.

Figure 12 shows the frequency of the wind speed greater than 5 m/s where red colour represents the frequency greater than 70%. Blue colour circles identify the inland high wind resource locations. In the figures, it can see that there were more low wind speed situations along the coast of Guangdong in 2004. However, this situation improved in 2005 and 2006. It also shows that along the coast of Guangdong, Zhanjiang, Shenquan and Jinghai (in the blue circles) seem to have high wind resource to build wind farms.

Figure 12. Frequency of wind speed greater than 5 m/s where red colour represents frequency greater than 70%. Blue colour circles identify onshore high wind resource locations.

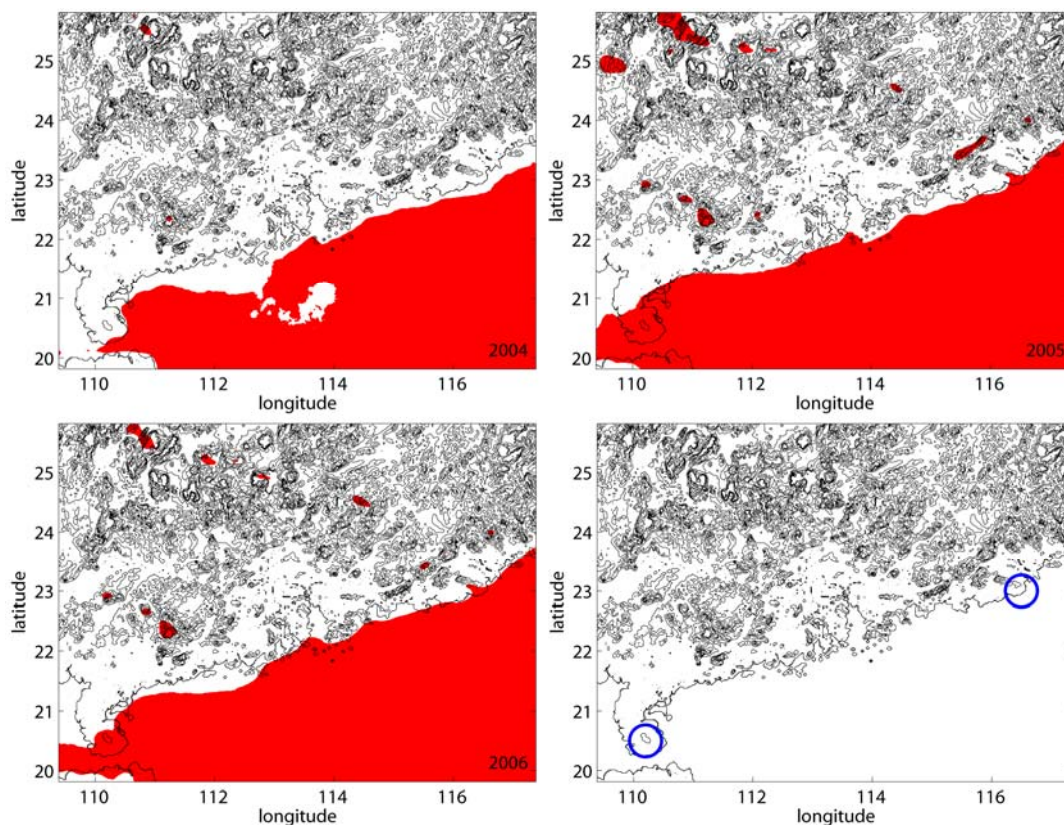


Table 2 and Table 3 (testing unassimilated data) show reasonable (satisfactory) agreement and the influence of the model-errors on the simulated wind power, on average, is 23%. But the question of whether it is good enough for wind power applications may still be open. Although this study demonstrates the use of MM5 and CALMET to generate a high-resolution wind field over Guangdong to investigate the wind power over the southern China, there is still a need for continuous improvements by incorporating with the urban canopy model [32] in our system for further study. Such incorporation would likely give a better representation of radiative exchange within the complex

urban canyon and give more detailed meteorological fields inside the roughness sublayer near and around urban areas, but it is less important for areas where wind turbines are likely. However, this kind of urban canopy model requires a whole new set of parameterizations and additional input data characterizing the canopies which are not yet available for southern China.

In addition, capacity factors, in practice, usually range from 20% to 70%, and mostly around 25-30%. The value of this factor is actually affected by the intermittent nature of the wind, the machine availability, and the turbine efficiency. It can also be influenced by other causes of loss of energy such as array interactions or transmission, which are not accounted for the machine performance characteristics [33,34]. Large energy investments and emissions attendant to intermittency, manufacture, transport and maintenance of wind farms should also not be overlooked [35,36].

4. Conclusions

Renewable energy resources have recently gained greater relevance in China, due to current excessive use of fossil fuel resources and the associated negative environmental impacts, such as air pollution, acid rain and the greenhouse effect. Increased cost of conventional energy resources, also have helped focus global attention on the development of renewable resources. Undoubtedly, wind power is likely to play a key role in the protection of our environment and will provide an efficient electricity source with a view to achieving sustainable development. In this paper it has successfully identified significant areas of high wind power potential in Guangdong Province.

A MM5/CALMET study of Guangdong Province was undertaken to examine the suitability of this approach for generating high resolution wind maps for the evaluation of wind power resources in an area with extremely complex topography and with relatively dense observational data available. MM5 was run in a nested mode with grid spacings of 40.5 km, 13.5 km, 4.5 km and 1.5 km. CALMET was run with grid spacings from 3 km for Guangdong Province to 100 m for Hong Kong. This combination of MM5 and CALMET was run for a study period of three years (2004-2006). The simulations did a very good job of replicating wind speeds at sites where the observation data were not assimilated into the CALMET simulations. The vertical performance of the simulation was very good compared with profiler observations. Our results indicate that utilizing a coarse prognostic meteorological model output as input for a diagnostic model provides an attractive option for generating accurate velocity fields for wind resource evaluations.

In this paper, it shows that almost 70% of the time in a year, the wind speed is over typical cut-in speed (~5 m/s) of the wind turbines. Because the power density is determined not only by the mean speed but also by the distribution of the wind speed, shape parameter (k) and scale parameter (c) over Guangdong Province are measured. Higher values of k (above 2) and c over there indicate that it has high wind power potential with stable wind availability. Thus, coastal regions in Guangdong Province have a high potential for the development of wind power resources. By examining the frequency of wind speed greater than 5 m/s, it also found that along the coast of Guangdong, Zhanjing, Shenquan and Jinghai seem to have high wind resource to build wind farms.

The diagnostic CALMET model alone contains limited physics in its formulation, and also depends upon the density, frequency, and accuracy of the observations used as input for computing wind fields. Based on this study, it appears that the hybrid approach of using a coarser MM5 run with a finer

CALMET run adequately represents meteorological conditions in complex terrain such as Pearl River Delta. However, the accuracy of the result will depend on the accuracy of the initial guess field of the MM5 simulation. It appears that whether CALMET is used or not, good model performance in areas of complex terrain requires that the prognostic model should be run at the highest possible horizontal resolution.

Acknowledgements

This work was supported by ITF, the China Light and Power Group, RGC grant NSFC/HKUST36, N_HKUST630/04 and NSFC Grant no. 49910161986. The authors would like to thank the following Government Departments for the provided data, the Hong Kong Observatory, the Environmental Protection Department, the Lands Department and the Planning Department.

References and Notes

1. WWEA. *WWEA Sustainability and Due Diligence Guidelines*. World Wind Energy Association, 2005. Available online: http://www.wwindea.org/home/images/stories/pdfs/wwea_05_11-10.pdf.
2. WWEA. *World Wind Energy Report 2008*. World Wind Energy Association, 2008. Available online: <http://www.wwindea.org/home/index.php>.
3. GWEC. *Global Wind 2008 Report*. Global Wind Energy Council, 2008. Available online: <http://www.gwec.net/>.
4. Fung, W.S. A feasibility study and engineering design of wind power in Hong Kong. Master Thesis, The Hong Kong Polytechnic University: Hong Kong, China, 1999.
5. Li, G. Feasibility of large-scale offshore wind power for Hong Kong - a preliminary study. *J. Renew. Energy* **2000**, *21*, 387-402.
6. Lu, L.; Yang H.X. Investigation on wind power potential on Hong Kong islands - an analysis of wind power and wind turbine characteristics. *J. Renew. Energy* **2002**, *27*, 1-12.
7. Zhou, W.; Yang, H.X.; Fang, Z.H. Wind power potential and characteristic analysis of the Pearl River Delta region, China. *J. Renew. Energy* **2006**, *31*, 739-753.
8. Dudhia, J. A nonhydrostatic version of the Penn State-NCAR Mesoscale Model: Validation tests and simulation of an Atlantic cyclone and cold front. *Mon. Wea. Rev.* **1993**, *121*, 1493-1513.
9. Grell, G.A.; Dudhia, J.; Stauffer, D.R. A description of the fifth generation Penn State-NCAR Mesoscale Model (MM5). *NCAR Tech. Note NCAR/TN-398 +STR* **1994**, 138-139.
10. Wang, X.M.; Lin, W.S.; YanG, L.M.; Deng, R.R.; Lin, H. A numerical study of influences of urban land-use change on ozone distribution over the Pearl River Delta region, China. *Tellus B* **2007**, *59*, 633.
11. Lin, C.Y.; Wang, Z.F.; Chou, C.C.K.; Chang, C.C.; Liu, S.C. A numerical study of an autumn high ozone episode over southwestern Taiwan. *J. Atmos. Environ.* **2007**, *41*, 3684-3701.
12. Wei, X.L.; Li, Y.S.; Lam, K.S.; Wang, A.Y.; Wang, T.J. Impact of biogenic VOC emissions on a tropical cyclone-related ozone episode in the Pearl River Delta region, China. *J. Atmos. Environ.* **2007**, *41*, 7851-7864.

13. Chune, S.; Fernando, H.J.S.; Wang, Z.F.; An, X.Q.; Wu, Q.Z. Tropospheric NO₂ columns over East Central China: Comparisons between SCIAMACHY measurements and nested CMAQ simulations. *J. Atmos. Environ.* **2008**, *42*, 7165-7173.
14. Huang, J.P.; Fung, J.C.H.; Lau, A.K.H.; Qin, Y. Numerical simulation and process analysis of typhoon-related ozone episodes in Hong Kong. *J. Geophys. Res.* **2005**, *110*, D05301.
15. Huang J.P.; Fung, J.C.H.; Lau, A.K.H. Integrated processes analysis and systematic meteorological classification of ozone episodes in Hong Kong. *J. Geophys. Res.* **2006**, *111*, D20309.
16. Hong, S.Y.; Pan, H.L. Nonlocal boundary layer vertical diffusion in a medium-range forecast model, *Mon. Weather Rev.* **1996**, *124*, 2322-2339.
17. Ding, A.; Wang, T.; Zhao, M.; Wang, T.; Li, Z. Simulation of sea-land breezes and a discussion of their implications on the transport of air pollution during a multi-day ozone episode in the Pearl River Delta of China. *J. Atmos. Environ.* **2004**, *38*, 6737-6750.
18. Seaman, N.L.; Stauffer, D.R.; Lario-Gibbs, A.M. A Multiscale Four- Dimensional Data Assimilation System Applied in the San Joaquin Valley during SARMAP. Part I: Modeling Design and Basic Performance Characteristics. *J. Appl. Meteorol.* **1995**, *34*, 1739-1761.
19. Fung, J.C.H.; Lau, A.K.H.; Lam, J.S.L.; Yuan, Z. Observational and modeling analysis of a severe air pollution episode in western Hong Kong. *J. Geophys. Res.* **2005**, *110*, D09105.
20. Douglas, S.G.; Kessler, R.C. *User's guide to the diagnostic wind model (Version 1.0)*. Systems Applications Inc.: San Rafael, CA, USA, **1988**.
21. Chandrasekar, A.; Philbrick, R.; Clark, B.; Doddridge, B.; Georgopoulos, P. Evaluating the performance of a computationally efficient MM5/CALMET system for developing wind field inputs to air quality models. *J. Atmos. Environ.* **2003**, *37*, 3267-3276.
22. Chuang, M.T.; Fu, J.S.; Jang, C.J.; Chan, C.C.; Ni, P.C.; Lee, C.T. Simulation of long-range transport aerosols from the Asian Continent to Taiwan by a Southward Asian high-pressure system, *Sci. Total Environ.* **2008**, *406*, 168-179.
23. Streets, D.G.; Fu, J.S.; Jang, C.J.; Hao, J.M.; He, K.B.; Tang, X.Y.; Zhang, Y.H.; Wang, Z.F.; Li, Z.P.; Zhang, Q.; Wang, L.T.; Wang, B.Y.; Yu, C. Air quality during the 2008 Beijing Olympic Games. *J. Atmos. Environ.* **2007**, *41*, 480-492.
24. Jackson, B.; Chau, D.; Gurer, K.; Kaduwela, A. Comparison of ozone simulations using MM5 and CALMET/MM5 hybrid meteorological fields for the July/August 2000 CCOS episode. *J. Atmos. Environ.* **2006**, *40*, 2812-2822.
25. Yim, S.H.L.; Fung, J.C.H.; Lau, A.K.H.; Kot, S.C. Developing a high-resolution wind map for a complex terrain with a coupled MM5/CALMET system. *J. Geophys. Res.* **2007**, *112*, D05106.
26. Truhetz, H.; Gobiet, A.; Kirchengast, G. Evaluation of a dynamic-diagnostic modeling approach to generate highly resolved wind climatologies in the Alpine region. *Meteorol. Z.* **2007**, *16*, 191-201.
27. Barna, M.B.; Lamb, B.K.; O'Neill, S.M.; Westberg, H.; Figueroa-Kaminsky, C.; Otterson, S.; Bowman, C.; DeMay, J. Modeling ozone formation and transport in the Cascadia region of the Pacific Northwest. *J. Appl. Meteorol.* **2000**, *39*, 349-366.
28. Lu, R.; Turco, R.P.; Jacobson, M.A. An integrated air pollution modeling system for urban and regional scales: 1. Simulations for SCAQS 1987. *J. Geophys. Res.* **1997**, *102*, 6063-6079.

29. Barna, M.B.; Lamb, B.K. Improving ozone modeling in regions of complex terrain using observational nudging in a prognostic meteorological model, *J. Atmos. Environ* **2000**, *34*, 4889-4906.
30. Weisser, D. A wind energy analysis of Grenada: An estimation using the 'Weibull' density function. *J. Renew. Energy* **2003**, *28*, 1803-1812.
31. Mukund, R.P. *Wind and Solar Power Systems*, 2nd ed.; CRC Press: Boca Raton, FL, USA., 2006.
32. Dupont, S.; Otte, T.; Ching, J. Simulation of meteorological fields within and above urban and rural canopies with a mesoscale model (MM5). *Boundary Layer Meteorol.* **2004**, *113*, 111-158.
33. Abderrazzaq, M.H. Energy production assessment of small wind farms. *J. Renew. Energy* **2004**, *29*, 2261-2272.
34. Walker, J.F.; Jenkins, N. *Wind energy technology*. John Wiley & Sons Inc: New York, NY, USA, 1997.
35. Ferguson, A.R.B. Wind Power: Benefits and Limitations. In *Biofuels, Solar and Wind as Renewable Energy Systems*; Springer: Dordrecht, the Netherlands, 2008; pp. 133-151.
36. Tyner, G., Sr. *Net Energy from Wind Power*. Minnesotans for Sustainability, 2002.

© 2009 by the authors; licensee Molecular Diversity Preservation International, Basel, Switzerland. This article is an open-access article distributed under the terms and conditions of the Creative Commons Attribution license (<http://creativecommons.org/licenses/by/3.0/>).